Electrochimica Acta 155 (2015) 201–208

Contents lists available at ScienceDirect

Electrochimica Acta

journal homepage: www.elsevier.com/locate/electacta

Tailoring of porous and nitrogen-rich carbons derived from hydrochar for high-performance supercapacitor electrodes

Feng Gao [a,b], Guanghua Shao [a], Jiangying Qu [a,b,*], Siyuan Lv [a], Yuqian Li [a], Mingbo Wu [c,**]

[a] Faculty of Chemistry and Chemical Engineering, Liaoning Normal University, Dalian, 116029, China
[b] Carbon Research Laboratory, Center for Nano Materials and Science, School of Chemical Engineering, State Key Lab of Fine Chemicals, Dalian University of Technology, Dalian, 116024, China
[c] State Key Laboratory of Heavy Oil Processing, China University of Petroleum, Qingdao, 266580, China

ARTICLE INFO

Article history:
Received 12 November 2014
Received in revised form 11 December 2014
Accepted 11 December 2014
Available online 15 December 2014

Keywords:
biomass
hydrochar
carbon
nitrogen doping
supercapacitor

ABSTRACT

Biomass-derived hydrochar (HC) was used as the precursor to synthesize porous and nitrogen-rich carbons for supercapacitor electrodes. Porous carbon (HC/KOH) activated by potassium hydroxide was used to prepare nitrogen-rich porous carbon (HC/KOH/N) by subsequent calcination in melamine. Similarly, HC/N/KOH was obtained from nitrogen-rich carbon (HC/N) calcined in melamine by subsequent KOH activation. It is found that KOH plays an important role on the creation of porous structures and selective production of active pyridinic and pyrrolic nitrogen species. HC/KOH samples with abundant pores are excellent as supercapacitor electrodes in basic medium, whereas HC/N/KOH samples enriched with nitrogen functionalities are especially applicable in acidic medium. Typically, HC/KOH and HC/N/KOH show the highest specific capacitance of 279 and 492 F g^{-1} at the current density of 0.1 A g^{-1} in KOH and H_2SO_4 electrolytes, respectively. Their specific energy density and power density are up to 8.1–12 Wh kg^{-1} and about 24 W kg^{-1} at 0.05 A g^{-1} in two-electrode cell. The excellent electrochemical properties of as-made carbons may be attributed to the high specific surface (1197 m^2 g^{-1}) for the former, and to the synergistic effect of combined accessible specific surface area (566 m^2 g^{-1}) and doped nitrogen (4.38 wt.%) for the latter. This research provides a new routine for the development of high-performance electrochemical supercapacitors with carbonaceous electrodes derived from biomass precursors.

1. Introduction

Electrochemical supercapacitors as power storage devices have exhibited many advantages including high power density, good reversibility and long cycle life, which enable wide applications in electric systems such as consumer electronics, energy management and mobile electrical system [1,2]. The charge storage mechanism of supercapacitors is based on the electrical double layer of electrodes (EDLCs) with high specific surface area, and/or based on the pseudocapacitance associated with fast surface redox reactions [3,4]. The electrode material is the key factor determining the capacitance performance of supercapacitors, of which porous carbons are the commonly used electrode materials [5–8]. Various carbon materials including activated carbon (AC), mesoporous carbon (MC), carbon nanotubes (CNTs) and graphene have been explored as electrode materials for EDLCs. Among them, ACs produced by different activation processes from various precursors are the most commonly used electrode materials because of their high specific capacitance and moderate cost [9]. In comparison with AC, template synthesized MC with regular structure and suitable pore size holds a great promise as supercapacitor electrodes due to its superior specific capacitance, approx. 100–300 F g^{-1} in aqueous medium and 50–150 F g^{-1} in organic medium [10–13]. Recently, CNTs with unique tubular porous structures and graphene with large specific surface have been widely used for electrode materials, however the high production cost limits their widespread use [14–18]. In contrast to EDLCs, some nitrogen doped (N-doped) carbons exhibit a pseudocapacitance related to charge or mass transfer between the electrodes and the electrolyte ions [19,20]. N-doped porous CNTs exhibit a reversible specific capacitance of 202 F g^{-1} at the current density of 1.0 A g^{-1} in 6.0 mol L^{-1} aqueous KOH electrolyte [21]. Similarly, N-rich nonporous carbons derived from melamine/mica composite have high volumetric capacitance, even reach 280 F cm^{-3} in KOH electrolyte and 152 F cm^{-3} in H_2SO_4 electrolyte [22]. Besides the

* Corresponding author. Tel.: +86 411 82158329.
** Corresponding author. Tel.: +86 532 86983452.
E-mail addresses: qujy@lnnu.edu.cn (J. Qu), wumb@upc.edu.cn (M. Wu).

http://dx.doi.org/10.1016/j.electacta.2014.12.069
0013-4686/

great efforts on the synthesis of carbon-based electrodes with good capacitive performance, the exploration of renewable carbonaceous raw materials is a much-needed tangible work considering the wide application of good performance supercapacitor with low cost.

Due to the cheap, abundant, and sustainable advantages, biomass-based carbon materials have been applied in the fields of catalysis, adsorbent and energy storage [23–28]. Recent researches demonstrate that carbohydrate dehydration via hydrothermal approach allows the production of novel carbon materials from natural precursors without toxic chemicals used [23,24]. The resulting solid carbons (named hydrochars, HCs for short) exhibit controllable size as well as high content of oxygen-containing functional groups [29,30], and have been used as catalyst supports, encapsulated nanoparticles and Li-storage materials [25,31]. Unfortunately, the HCs generally possess a low surface area (less 20 $m^2 g^{-1}$) and low porosity, which potentially limit their practical applications. It is known that physical or chemical activation on HCs can produce pores as well as functional groups. HCs have also been reported as the precursor for porous carbons used as anode materials in supercapacitor. For example, microporous carbons with high specific surface area and pore volume derived from HCs exhibit a specific capacitance of up to 236 $F g^{-1}$ in a symmetric two-electrode system [32,33]. Similarly, porous N-doped carbons produced by hydrothermal carbonization of D-glucosamine followed by chemical activation also show the superior performance in supercapacitors [34]. Based on the reports, the activation and N-doping of hydrochars are very crucial to yield the electroactive materials. Thus the need to explore effective way to modify hydrochars for supercapacitor application leads to a deep-exploration of this field.

Herein, we present an effectively chemical activation process to synthesize porous and N-rich carbons using hydrochar as carbon source. This chemical activation can be easily accomplished by KOH activation and/or melamine treatment in different sequences. The synthesis of carbons based on the chemical treatment and their electrochemical performances are detailed discussed in the present paper.

2. Experimental

2.1. Synthesis of HCs

2.28 g commercial glucose (purchased from Shanghai, China) was sufficiently dissolved in 23 mL distilled water to form a clear solution. The solution was then transferred to a 30 mL Teflon-sealed autoclave, sealed and then treated at 180 °C for 7 h. The puce product was separated by 5 cycles of centrifugation, cleaned by washing, and dried at 80 °C. The obtained HCs were used as carbon precursor for further chemical activation. For comparison, HC was calcined in N_2 at 800 °C for 1 h to yield HC-800 sample.

2.2. Synthesis of KOH activated carbons (HC/KOH)

HC was impregnated in 2 M KOH solution for 12 h with 1:2 of the mass ratio of HC to KOH. The resultant material was dried at 80 °C, followed by calcination at 800 °C for 1 h with a heating rate of 5 °C min^{-1} in argon. The sample was designated as HC/KOH after removal of the residues by sufficient washing and drying at 80 °C.

2.3. Synthesis of N-doped carbons (HC/N)

Melamine was used as nitrogen donor to prepare N-doped carbons. The mixture with 1:5 of the weight ratio between HC and melamine was fully ground followed by calcination at 800 °C for 1 h with a heating rate of 5 °C min^{-1} in argon ambient. Finally, the sample left in the furnace was denoted as HC/N.

2.4. Synthesis of both N-doped and KOH activated carbons (HC/N/KOH and HC/KOH/N)

The synthesis process of HC/N/KOH sample was similar to that of above HC/KOH sample (see Section 2.2), the only difference was HC/N instead of HC as carbon source. HC/KOH/N sample was also similarly synthesized as HC/N sample (see Section 2.3) by using HC/KOH sample instead of HC as carbon precursor.

2.5. Measurements

The electrochemical properties of as-obtained samples were investigated using a three-electrode cell configuration at room temperature. The working electrodes were fabricated by mixing the prepared powders with 10 wt% acetylene black and 5 wt% polytetrafluoroethylene (PTFE) binder. A small amount of ethanol was added to the mixture to produce a homogeneous paste. The mixture was pressed onto nickel foam (in KOH solution) or titanium mesh (in H_2SO_4 solution) current-collector (1.5 cm in diameter) to make electrodes. The mass of the active materials was in a range of 3–5 mg per electrode, and the thickness of the electrodes was about 100 μm. Before the electrochemical test, the as-prepared electrode was soaked overnight in a 6 M KOH or 1 M H_2SO_4 solution. Platinum foil and Hg/HgO electrode or Hg/Hg_2SO_4 electrode were used as the counter and reference electrodes, respectively. Furthermore, two identical electrodes were used for the test in 2-electrode symmetric cell configuration with about 3.5 mg active materials on one electrode. The cyclic voltammetry (CV) measurement was conducted on a LK2005A electrochemical workstation (Tianjin Lanlike Company, China). The galvanostatic charge-discharge measurement was performed on a Land CT2001A cycler at room temperature (Wuhan Land Instrument Company, China).

The morphologies and structures of the as-obtained products were examined using field emission scanning electron microscopy (SEM, Hitachi Ltd SU8010), X-ray photoelectron spectroscopy (XPS, Thermo VG Scientific Sigma Probe spectrometer) and elemental analysis (Elemental Analyzer Vario EL III). The Brunauer-Emmett-Teller (BET) surface area of as-synthesized samples was determined by physisorption of N_2 at 77 K using a Micromeritics ASAP 2020 analyzer.

3. Results and discussion

The synthesis of porous and N-doped porous carbons using HCs as carbon precursor was described in Fig. 1. Firstly, HCs were hydrothermally produced at 180 °C from glucose, then the resultant HCs were annealed at 800 °C after mixing with melamine

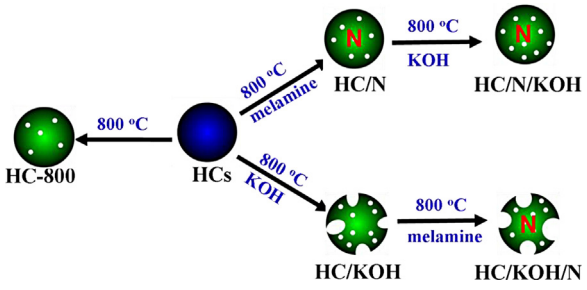

Fig. 1. Schematic illustration of chemically modified carbons by different chemical routes using HCs as the carbon precursor.

and/or KOH. The resultant carbons were labeled according to the different chemical processes: HC/N (melamine treatment on HCs), HC/KOH (KOH activation on HCs), HC/N/KOH (KOH activation on HC/N sample) and HC/KOH/N (melamine treatment on HC/KOH sample). For comparison, HC-800 was also obtained after calcination of HCs at 800 °C in the absence of both melamine and KOH.

SEM images of carbons derived from HCs are shown in Fig. 2. HC-800 sample exhibits a spherical shape with the uniform diameter of about 500 nm (Fig. 2a). The resulting HC/N and HC/N/KOH also show the similar morphology like HC-800 (Figs. 2b and 2c), revealing little variation in shapes regardless of the melamine treatment, even after the subsequent KOH activation. However, the morphologies of HC/KOH and HC/KOH/N both firstly activated by KOH are very different from that of HC-800, where the compact networks of intercalated particles instead of sphere morphologies are given in Figs. 2d and 2e. Such results indicate that KOH can etch the sphere-like HCs and create a rough surface with many small pores. Remarkably, the resulting carbons are decorated with disordered meso/micorpores (see the inset images of Figs. 2c and 2e), which would play an important role in charge accommodation for supercapacitor application [35].

To further investigate the porosity of the resulting carbons after different treatments, N_2 sorption isotherms are shown in Fig. 3A. It is observed that HC-800 sample exhibits type II isothermal, while the other samples display combined type I/IV sorption isotherms. Detailed information on the BET surface area (S_{BET}) and pore size distributions of all samples are summarized in Table 1. It is found that the structural characters of the samples are seriously affected by the synthetic conditions. HC-800 shows a S_{BET} of 75 $m^2 g^{-1}$, while nonporous HC displays a very low S_{BET} about 11 $m^2 g^{-1}$ in this case. Such increased surface area of HC-800 can be attributed to the creation of porosity by decomposition of the abundant functional groups (such as ethers, carbonyl and carboxylic groups) in HC [36,37]. Porosity is greatly developed during melamine treatment and/or KOH activation of HCs. In case of melamine treatment, the S_{BET} of HC/N increases to 148 $m^2 g^{-1}$, which is almost twice that of HC-800. Furthermore, HC/N/KOH activated by KOH from HC/N shows larger S_{BET} of 566 $m^2 g^{-1}$ than 148 $m^2 g^{-1}$ of HC/N. Similarly, S_{BET} values of HC/KOH and HC/KOH/N have respectively been increased to 1197 and 341 $m^2 g^{-1}$. It is obvious that KOH activation plays an important role on the creation of porosity due to the oxidation of carbons [38,39]. The change of pore volume for the obtained samples follows the same order as their surface area. Besides, the pore sizes of the resultant samples are centered at 1∼10 nm. It is believed that the coexistence of micro/meso-scale pores is required for rapid ion transport and high power characteristic of supercapacitors [35].

To confirm the influence of chemical activation process on the composition of the synthesized carbon samples, XPS and element analyses were conducted. Table 2 shows the contents of nitrogen, carbon and oxygen in the resultant samples obtained from elemental analyses. Carbon content decreases from 90.1% for HC-800 to 85.6% for HC/KOH. Such variation in carbon content is ascribed to the reaction between HC and KOH as followed [38]:

$$6KOH + 2C = 2K + 3H_2 + 2\ K_2CO_3$$

The relative quantities of nitrogen-containing groups for the resultant samples differ after treatment with melamine [40]. The content of nitrogen in HC/N is particularly high (19.2 wt.%), which clearly proves that it is an effective method to dope nitrogen into carbon materials with melamine as the nitrogen source. However, the nitrogen contents are relatively low for HC/N/KOH (4.38 wt.%) and HC/KOH/N (3.28 wt.%). Obviously, further KOH activation can significantly decrease the nitrogen content of the samples.

XPS spectra of N-doped HC/N, HC/N/KOH and HC/KOH/N samples are presented in Fig. 4 and corresponding data are summaried in Table 2. The N 1 s spectra are deconvoluted into four different types of nitrogen functionalities [22], representing pyridinic N (N-6 at 398.0 eV), pyrrolic/pyridonic N (N-5 at 399.7 eV), quaternary N (N-Q at 400.8 eV) and oxidized N (N-X at 402.5 eV) [41]. Among them, N-5 and N-6 forms with planar structures are found generally more active than N-Q and N-X forms with 3D structures in supercapacitor [40,41]. For comparison, the quantitative analyses of three carbon samples are listed in Table 2. The amount of 3D nitrogen species (N-X and N-Q forms) is significantly high in HC/N sample with 33.3 and 18.9 at.%, respectively, whereas planar N species (N-5 and N-6) only account

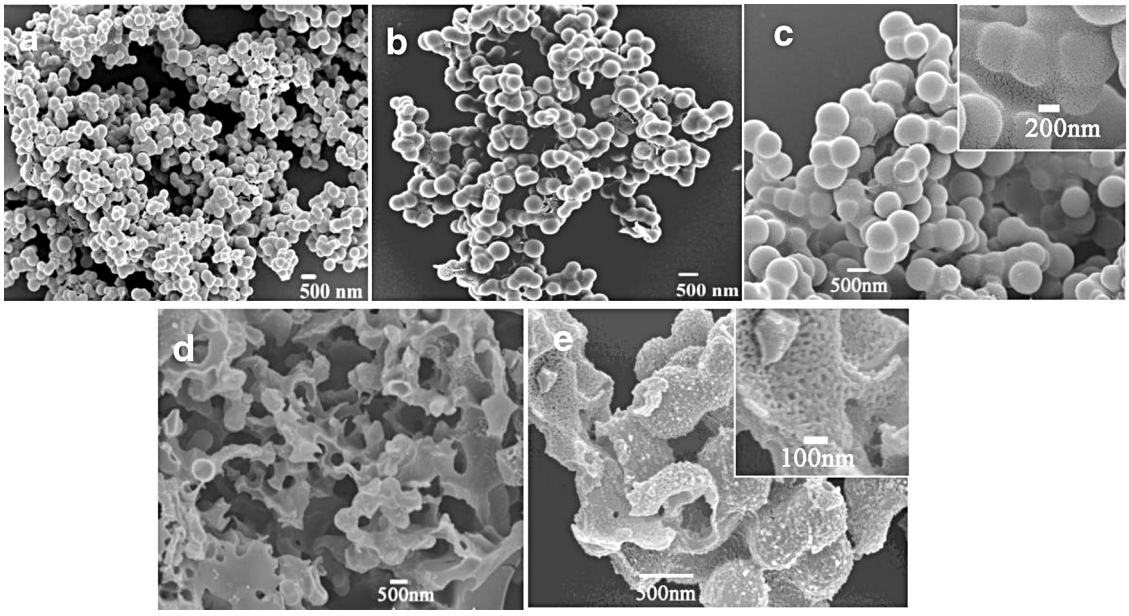

Fig. 2. SEM images of (a) HC-800, (b) HC/N, (c) HC/N/KOH, (d) HC/KOH, (e) HC/KOH/N. Insets are their corresponding magnified images.

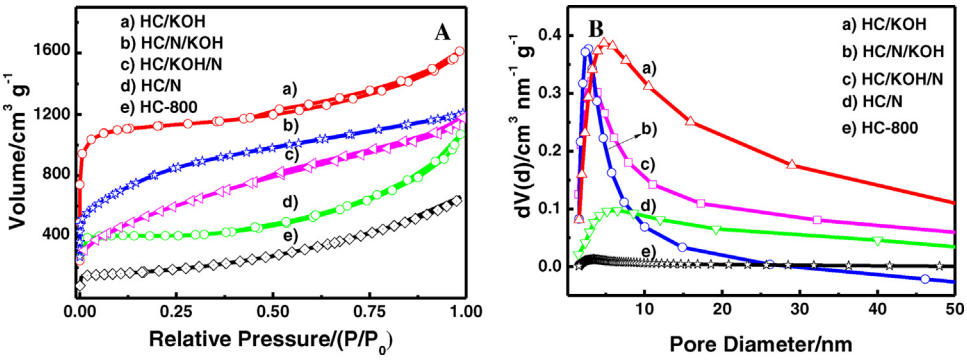

Fig. 3. Nitrogen adsorption and desorption isotherms (A) and corresponding pore size distribution curves (B) of (a) HC/KOH, (b) HC/N/KOH, (c) HC/KOH/N, (d) HC/N and (e) HC-800.

Table 1
Porous properties of chemically modified carbons derived from HCs.

Sample	S_{BET} ($m^2 g^{-1}$)	S_{mic} ($m^2 g^{-1}$)	V_{total} ($cm^3 g^{-1}$)	V_{mic} ($cm^3 g^{-1}$)	Pore size (nm)
HC-800	75	23	0.10	0.09	1.5∼4.0
HC/KOH	1197	928	0.74	0.48	1.3∼8.0
HC/N	148	109	0.15	0.07	1.5∼10
HC/N/KOH	566	255	0.27	0.21	1.4∼7.5
HC/KOH/N	341	123	0.19	0.14	1.4∼7.5

for 47.8% of the N species. Comparing with HC/N, HC/N/KOH has lower N content, indicating that KOH activation largely reduces the N content in HC/N/KOH. Furthermore, it is noted that N components of HC/N and HC/N/KOH are obviously different. HC/N/KOH contains more N-5 (58.3 at.%) and less N-X (3.8 at.%) functional groups, and its planar-N species amount for 69.4 at.% of the N species. Similarly, the planar N content in HC/KOH/N is as high as 75.8 at.%. These data suggest that the active N species, that are pyridinic N and pyrrolic N species, are produced selectively after KOH activation of the carbons. The relevant work need to be further developed.

The electrochemical measurements of all obtained carbons were performed in both basic (6 M KOH) and acidic (1 M H_2SO_4) electrolytes using three-electrode cells (Fig. 5 and Fig. 6). Cyclic voltammetry (CV) shows a rectangular-like shape in KOH electrolyte (Fig. 5a) and obvious redox peaks appear for HC/N/KOH sample in H_2SO_4 electrolyte at a scan rate of 5 mV s^{-1} (Fig. 6a). Such obvious change on the CV curves in acidic electrolyte is probably ascribed to the basic character of nitrogen functionalities in N-modified carbon material. However, the nitrogen doping nature is not the definitive factor for the induced capacitance. As HC/N is concerned, its redox peaks with the highest nitrogen content in all samples are weak and its CV curve is rectangular-like. Furthermore, the capacitances of the carbon samples in KOH electrolyte decrease qualitatively in the following order: HC/KOH > HC/N/KOH > HC/KOH/N > HC/N > HC-800. This result is in good agreement with the order of the surface areas as well as the pore volumes of these samples, highlighting the advantage of the accessible porous structures for enhanced capacitance [38].

The galvanostatic charge/discharge curves at a current density of 200 mA g^{-1} were used to characterize the capacitive properties of carbon samples, as shown in Figs. 5b and 6b. The distorted linear shapes of carbon samples in H_2SO_4 electrolyte indicate the presence of pseudocapacitance, which is consistent with the CV results. In both acidic and basic electrolytes, HC-800 with low specific surface area and without nitrogen functionality exhibits the poor electrochemical capacitance. Figs. 5c and 6c give the relationships between specific capacitances (*Cs*) and current densities. The *Cs* is calculated according to $Cs = I \times \Delta t/(\Delta V \times m)$ from the discharge curves, where I is the constant discharge current, Δt is the discharge time, ΔV is the potential drop during discharge time, and m is the total mass of the active electrode materials. Over the current density in the range from 0.05 to 3 A g^{-1} in 6 M KOH electrolyte (Fig. 5c), the charge storage capacities of the obtained samples quantitatively decrease in the following order: HC/KOH > HC/N/KOH > HC/KOH/N > HC/N > HC-800, and are 279, 261, 249, 193, 16 F g^{-1} at the current density of 0.1 A g^{-1}. Such performances are in agreement with the character of the hierarchical porous structures of those carbons, where the larger the specific surface area is, the higher the charge storage capacity

Table 2
The contents of nitrogen, carbon and oxygen in the obtained samples from elemental analysis (wt.%) and XPS analysis (at.%).

Sample	N (wt.%)	C (wt.%)	O (wt.%)	pyridinic [N-6, at.%] 398.0 eV	pyrrolic [N-5, at.%] 399.7 eV	quaternary [N-Q, at.%] 400.8 eV	oxidized [N-X, at.%] 402.5 eV
HC-800	0	90.1	8.35	–	–	–	–
HC/KOH	0	85.6	12.5	–	–	–	–
HC/N	19.2	59.9	19.9	30.3	17.5	18.9	33.3
HC/N/KOH	4.38	83.3	11.1	11.1	58.3	26.8	3.80
HC/KOH/N	3.28	88.4	7.06	28.5	47.3	17.1	7.10

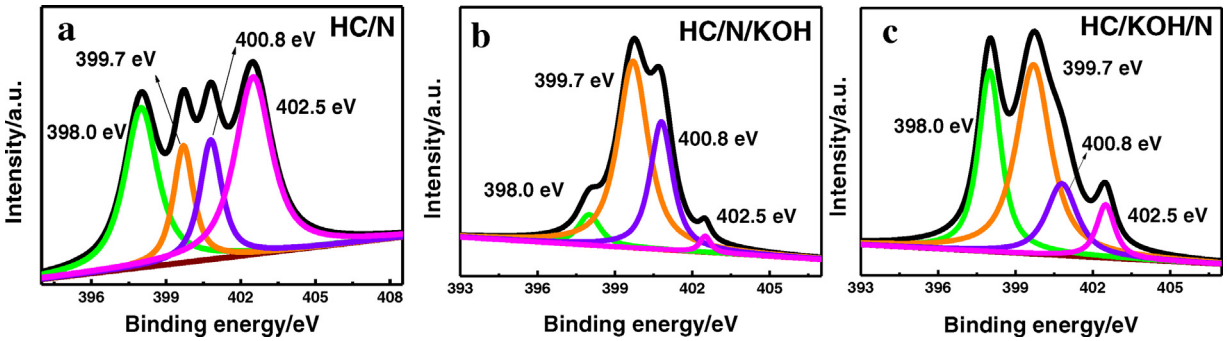

Fig. 4. XPS spectra and the corresponding N1 s deconvolution of melamine-treated samples: (a) HC/N, (b) HC/N/KOH, and (c) HC/KOH/N.

is. Thus, HC/KOH sample with the largest surface area (1197 $m^2 g^{-1}$) and pore volume (0.74 $cm^3 g^{-1}$) presents the highest performance for 375, 279, 255, 243, 237, 234 and 231 $F g^{-1}$ at the current density of 0.05, 0.1, 0.2, 0.5, 1.0, 2.0 and 3.0 $A g^{-1}$, respectively. The excellent high rate performance of the resultant carbon is attributed to its hierarchical porous structures (as shown in Fig. 2 and Fig. 3) that facilitate rapid electrolyte transfer. In contrast, the *Cs* of carbon samples has changed in acidic electrolyte as follow: HC/N/KOH > HC/KOH > HC/N > HC/KOH/N > HC-800, and are 492, 332, 238, 123, 11 $F g^{-1}$ at the current density of 0.1 $A g^{-1}$, respectively. Although HC/N/KOH sample has much lower specific surface area than that of HC/KOH, it has a larger capacitance, which is contributed by the induced pseudocapacitance brought by its N-rich functionalities. Such pseudocapacitance is due to the redox reactions of electrochemically active nitrogen functionalities on the carbon surface, *e.g.* $>C{=}NH + 2e^- + 2H^+ \leftrightarrow >CH\text{-}NH_2$ [22]. With moderate surface area (566 $m^2 g^{-1}$) and suitable N content (4.38 wt.% N), HC/N/KOH sample exhibits the highest capacity among all samples in acid electrolyte. Its specific capacitances are 570, 492, 430, 363, 332, 322 and 313 $F g^{-1}$ at current densities of 0.05, 0.1, 0.2, 0.5, 1.0, 2.0 and 3.0 $A g^{-1}$, respectively. These values are significantly higher than that of previously reported N-doped hydrothermal carbons (300 $F g^{-1}$ at 0.1 $A g^{-1}$) [34], activated carbon (250 $F g^{-1}$ at 0.05 $A g^{-1}$) [40], and mesoporous N-rich carbon (305 $F g^{-1}$ at 0.2 $A g^{-1}$) [42]. The superior electrochemical performance suggests that both nitrogen functionalities and porous structure of the obtained carbons are favorable for their applications in supercapacitors. Besides the nitrogen functionalities and porous structure of carbon materials, the pore size distribution may also play roles in the electrochemical performance, which needs to be done in our lab in the near future.

To further understand the capacitive behaviors of the carbon samples, their electrochemical impedance spectroscopy (EIS) plots in H_2SO_4 electrolyte are given in Fig. 6d. The resulting Nyquist plots exhibit semicircles in the high-frequency region, reflecting the existence of the charge transfer resistance [43]. The diameters of the semicircles are listed in the following order: HC/N > HC/N/KOH > HC/KOH/N > HC/KOH. Such decreased diameters are in line with the reduced content of nitrogen functionalities, indicating a decreasing trend of charge transfer resistance. Similarly, the

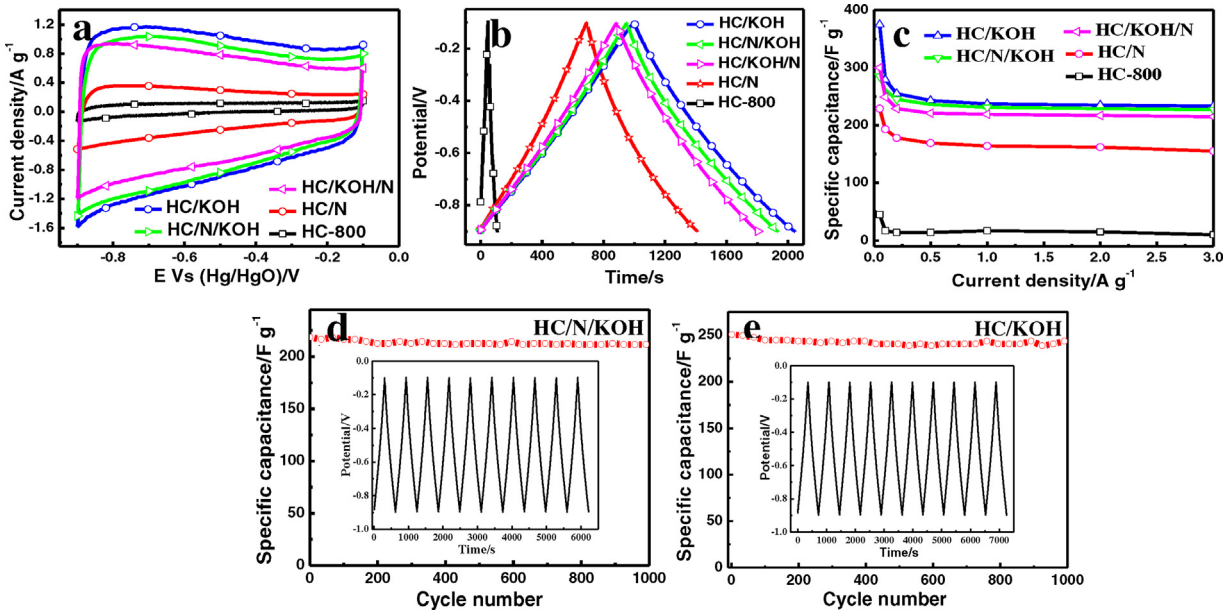

Fig. 5. Electrochemical performances of different carbon samples measured in a three-electrode system in 6 M KOH electrolyte: (a) cyclic voltammograms of carbon samples at the scan rate of 5 mV s^{-1}, (b) charge-discharge curves of carbon samples at the current density of 200 mA g^{-1}, (c) specific capacitances of carbon samples at different current densities, (d, e) cycling performances of HC/N/KOH and HC/KOH samples for 1000th cycles loaded at a current density of 1 g^{-1}. The insets in Figs. 5d and e show the last 10 cycles of galvanostatic charge-discharge.

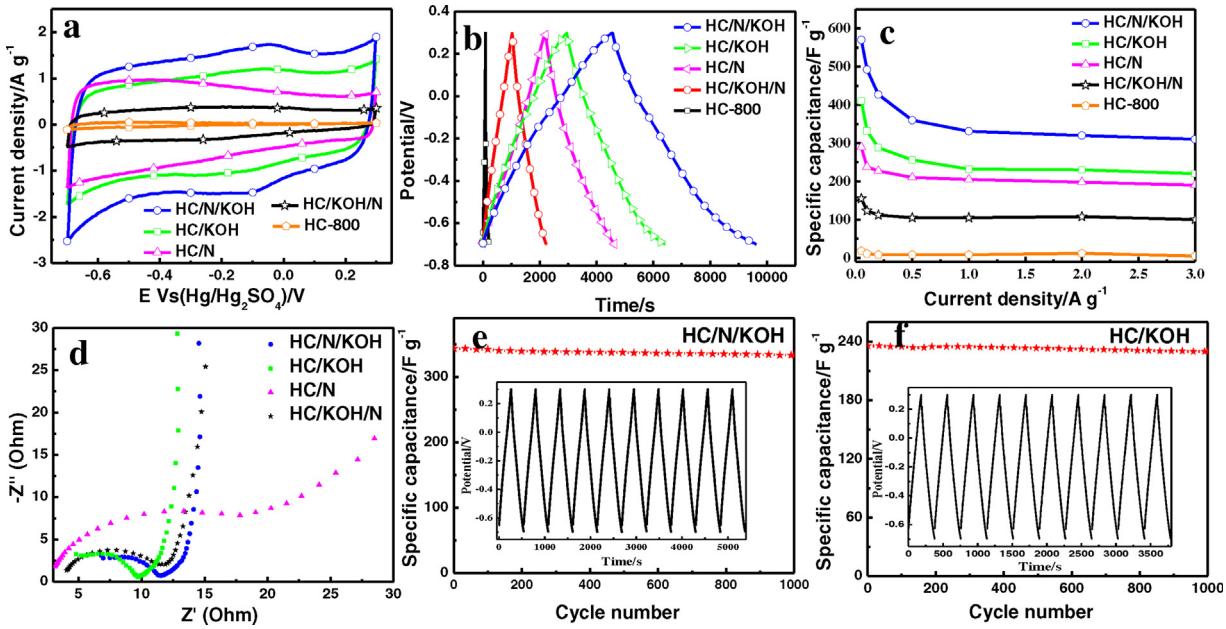

Fig. 6. Electrochemical performances measured in a three-electrode system in 1 M H2SO4 electrolyte: (a) cyclic voltammograms of carbon samples at the scan rate of 5 mV s^{-1}, (b) charge-discharge curves of carbon samples at the current density of 200 mA g^{-1}, (c) specific capacitances of carbon samples at different current densities, (d) Nyquist plots of various carbon samples, (e, f) the cycling performance of HC/N/KOH and HC/KOH for 1000th cycles loaded at 1 A g^{-1}. The insets in Figs. 6e and f show the last 10 cycles of galvanostatic charge-discharge.

deviation in slope at very low frequency might derive from the contribution of pseudocapacitance, in accordance with their nitrogen-doping nature [9].

The cycling stability of HC/N/KOH and HC/KOH electrodes are evaluated by galvanostatic charge/discharge curves at a current density of 1 A g^{-1} for 1000 cycles, as shown in Figs. 5d-e and Figs. 6e-f. In a three-electrode testing cell, the capacitance retentions for HC/N/KOH and HC/KOH electrodes are 97∼98% in both basic and acidic electrolytes, demonstrating the long-term stability of the carbon electrodes, and good futures as electrodes for supercapacitors.

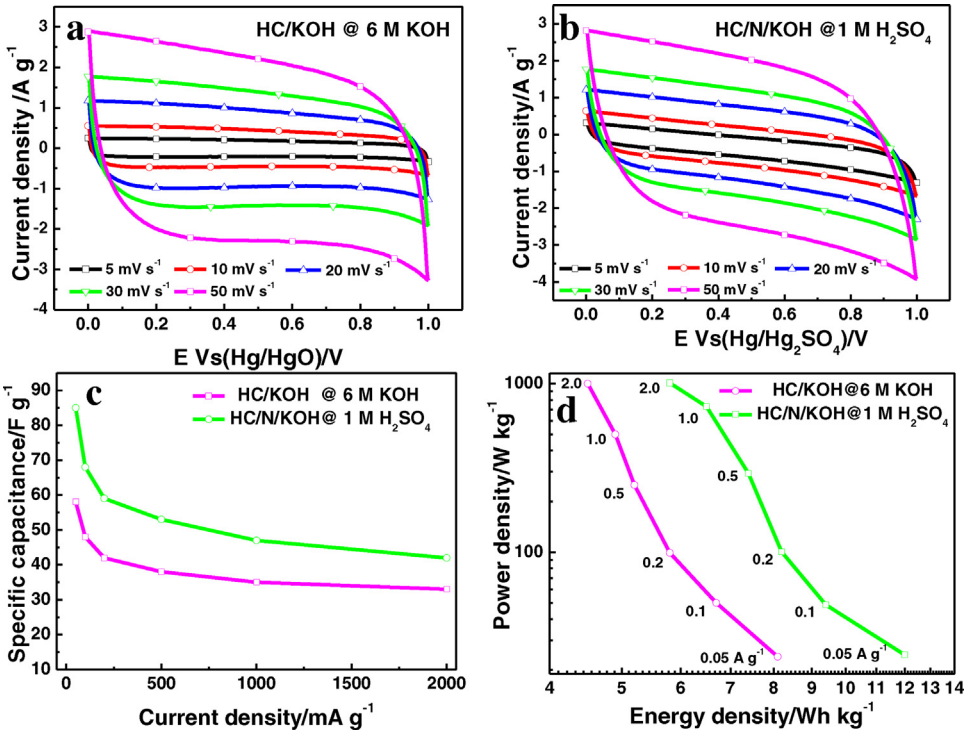

Fig. 7. Electrochemical performances of HC/KOH and HC/N/KOH samples for supercapacitor in a two-electrode symmetric cell configuration in 6 M KOH and 1 M H2SO4, respectively. (a, b) Cyclic voltammograms of HC/KOH in 6 M KOH and HC/N/KOH in 1 M H2SO4 at different scan rates; (c) Specific capacitances of HC/KOH and HC/N/KOH samples at different current density; (d) Power density of HC/KOH and HC/N/KOH samples vs. average energy density.

The best performance samples (HC/KOH and HC/N/KOH) have also been tested in a two electrode symmetric cell configuration in 6 M KOH and 1 M H_2SO_4 electrolyte, respectively. Figs. 7a and 7b exhibit the CV curves of both samples at different scan rates. Their rectangular-like shapes indicate a good capacitive behavior from 0 to 1 V over a wide range of voltage scan rates. The current density dependence of the specific capacitance is given in Fig. 7c. The specific capacitance obtained in the symmetric cell configuration is much lower than that obtained from 3-electrode setup [44]. Based on the total mass of two electrodes, the specific capacitance of HC/KOH and HC/N/KOH materials maintain specific capacitances of 58 and 85 $F g^{-1}$ at 0.05 $A g^{-1}$, respectively. The specific energy density of the two-electrode cell constructed reaches 8.1 $Wh kg^{-1}$ for HC/KOH and 12 $Wh kg^{-1}$ for HC/N/KOH at 0.05 $A g^{-1}$, whereas their specific power density is up to 24 and 24.6 $W kg^{-1}$, respectively. The average power density of the samples increases as the current density increases, and it reaches 1000 $W kg^{-1}$ for HC/KOH and 1008 $W kg^{-1}$ for HC/N/KOH at 2 $A g^{-1}$. A literature survey reveals that the performances of our materials are comparative to other carbon materials including mesoporous carbons and carbon nanotubes under the same measurement conditions [45,46].

4. Conclusion

Porous and N-rich carbons with high electrochemical performance were prepared from cheap hydrochars. Serial carbons with different porous structures and nitrogen contents were produced from hydrochars by chemical activation with KOH as the active agent and melamine as the nitrogen source. It is found that KOH plays an important role on the creation of porous structures and selective production of active pyridinic nitrogen and pyrrolic nitrogen species in the resultant carbons. Porous carbons with a large specific surface area and a high N-content are demonstrated the high electrochemical performance. Depending on the N-doped nature and/or porous structures, capacities of 11–570 $F g^{-1}$ are achieved for the obtained carbon samples. HC/KOH with the largest specific surface area (1197 $m^2 g^{-1}$) shows the outstanding specific capacitance in the wide range of charge-discharge rates and the highest electrochemical stability in KOH electrolyte, while HC/N/KOH exhibits the highest capacitive performance in H_2SO_4 electrolyte presumably because of the synergistic effect of moderate surface area (566 $m^2 g^{-1}$) and suitable nitrogen content (4.38% N). Their specific energy density and power density are up to 8.1–12 $Wh kg^{-1}$ and about 24 $W kg^{-1}$ at 0.05 $A g^{-1}$ in two-electrode cell. The specific capacitances of as-made HC/N/KOH and HC/KOH samples are obviously superior to those of reported carbonaceous materials. Furthermore, HC/N/KOH and HC/KOH samples exhibit excellent high rate performance and long cycle life. The porous and N-doped carbons prepared from hydrochar via a simple and cheap process, might be promising electrode materials for high-performance supercapacitors.

Acknowledgements

This work is supported by the NSFC (Nos. 51372277, 50902066), China Postdoctoral Science Foundation (2013M530922, 2014T70253) and Program for Liaoning Excellent Talents in University (LJQ2014118).

References

[1] P. Simon, Y. Gogotsi, Materials for electrochemical capacitors, Nat. Mater. 7 (2008) 845.
[2] M.H. Ervin, L.T. Le, W.Y. Lee, Inkjet-printed flexible graphene-based supercapacitor, Electrochim. Acta 147 (2014) 610.
[3] P. Ahuja, V. Sahu, S.K. Ujjain, R.K. Sharma, G. Singh, Performance evaluation of asymmetric supercapacitor based on cobalt manganite modified graphene nanoribbons, Electrochim. Acta 146 (2014) 429.
[4] D.S. Patil, S.A. Pawar, R.S. Devan, M.G. Gang, Y.-R. Ma, J.H. Kim, P.S. Patil, Electrochemical supercapacitor electrode material based on polyacrylic acid/polypyrrole/silver composite, Electrochim. Acta 105 (2013) 569.
[5] K. Xie, X.T. Qin, X.Z. Wang, Y.N. Wang, H.S. Tao, Q. Wu, L.J. Yang, Z. Hu, Carbon nanocages as supercapacitor electrode materials, Adv. Mater. 24 (2012) 347.
[6] Y.P. Zhai, Y.Q. Dou, D.Y. Zhao, P.F. Fulvio, R.T. Mayes, S. Dai, Carbon materials for chemical capacitive energy storage, Adv. Mater. 23 (2011) 4828.
[7] U.B. Nasini, V.G. Bairi, S.K. Ramasahayam, S.E. Bourdo, T. Viswanathan, A.U. Shaikh, Phosphorous and nitrogen dual heteroatom doped mesoporous carbon synthesized via microwave method for supercapacitor application, J. Power Sources 250 (2014) 257.
[8] H. Jiang, P.S. Lee, C.Z. Li, 3D carbon based nanostructures for advanced supercapacitors, Energ Environ. Sci. 6 (2013) 41.
[9] H. Zhu, X. Wang, X. Liu, X. Yang, Integrated synthesis of poly(o-phenylenediamine)-derived carbon materials for high performance supercapacitors, Adv. Mater. 24 (2012) 6524.
[10] W. Xing, S.Z. Qiao, R.G. Ding, F. Li, G.Q. Lu, Z.F. Yan, H.M. Cheng, Superior electric double layer capacitors using ordered mesoporous carbons, Carbon 44 (2006) 216.
[11] Z.B. Lei, D. Bai, X.S. Zhao, Improving the electrocapacitive properties of mesoporous CMK-5 carbon with carbon nanotubes and nitrogen doping, Microporous Mesoporous Mater. 147 (2012) 86.
[12] Z.J. Fan, Y. Liu, J. Yan, G.Q. Ning, Q. Wang, T. Wei, L.J. Zhi, F. Wei, Template-directed synthesis of pillared-porous carbon nanosheet architectures: high-performance electrode materials for supercapacitors, Adv. Energy Mater. 2 (2012) 419.
[13] Z.B. Lei, N. Christov, L.L. Zhang, X.S. Zhao, Mesoporous carbon nanospheres with an excellent electrocapacitive performance, J. Mater. Chem. 21 (2010) 2274.
[14] H. Pan, J.Y. Li, Y.P. Feng, Carbon nanotubes for supercapacitor, Nanoscale Res. Lett. 5 (2010) 654.
[15] A. Izadi-Najafabadi, S. Yasuda, K. Kobashi, T. Yamada, D.N. Futaba, H. Hatori, M. Yumura, S. Iijima, K. Hata, Extracting the full potential of single-walled carbon nanotubes as durable supercapacitor electrodes operable at 4 V with high power and energy density, Adv. Mater. 22 (2010) E235.
[16] Y.Q. Su, Q.O. Wu, G.Q. Shi, Graphene based new energy materials, Energy Environ. Sci. 4 (2011) 1113.
[17] J.T. Zhang, J.W. Jiang, H.L. Li, X.S. Zhao, A high-performance asymmetric supercapacitor fabricated with graphene-based electrodes, Energ Environ. Sci. 4 (2011) 4009.
[18] X. Yang, C. Cheng, Y. Wang, L. Qiu, D. Li, Liquid-mediated dense integration of graphene materials for compact capacitive energy storage, Science 341 (2013) 534.
[19] X. Zhao, A. Wang, J. Yan, G. Sun, L. Sun, T. Zhang, Synthesis and electrochemical performance of heteroatom-incorporated ordered mesoporous carbons, Chem. Mater. 22 (2010) 5463.
[20] F.B. Su, C.K. Poh, J.S. Chen, G.W. Xu, D. Wang, Q. Li, J.Y. Lin, X.W. Lou, Nitrogen-containing microporous carbon nanospheres with improved capacitive properties, Energ Environ. Sci. 4 (2011) 717.
[21] L.F. Chen, X.D. Zhang, H.W. Liang, M.G. Kong, Q.F. Guan, P. Chen, Z.Y. Wu, S.H. Yu, Synthesis of nitrogen-doped porous carbon nanofibers as an efficient electrode material for supercapacitors, ACS. Nano. 6 (2012) 7092.
[22] D. Hulicova-Jurcakova, M. Kodama, S. Shiraishi, H. Hatori, Z.H. Zhu, G.Q. Lu, Nitrogen-enriched nonporous carbon electrodes with extraordinary supercapacitance, Adv. Funct. Mater. 19 (2009) 1800.
[23] B. Hu, K. Wang, L.H. Wu, S.H. Yu, M. Antonietti, M.M. Titirici, Engineering carbon materials from the hydrothermal carbonization process of biomass, Adv. Mater. 22 (2010) 813.
[24] M. Sevilla, A.B. Fuertes, The production of carbon materials by hydrothermal carbonization of cellulose, Carbon 47 (2009) 2281.
[25] M. Soorholtz, R.J. White, T. Zimmermann, M.M. Titirici, M. Antonietti, R. Palkovits, F. Schuth, Direct methane oxidation over Pt-modified nitrogen-doped carbons, Chem. Commun. 49 (2013) 240.
[26] E. Raymundo-Pinero, M. Cadek, F. Beguin, Tuning carbon materials for supercapacitors by direct pyrolysis of seaweeds, Adv. Funct. Mater. 19 (2009) 1032.
[27] A. Chiappone, F. Bella, J.R. Nair, G. Meligrana, R. Bongiovanni, C. Gerbaldi, Structure–performance correlation of nanocellulose-based polymer electrolytes for efficient quasi-solid DSSCs, ChemElectroChem 1 (2014) 1350.
[28] R.J. White, M. Antonietti, M.M. Titirici, Naturally inspired nitrogen doped porous carbon, J. Mater. Chem. 19 (2009) 8645.
[29] D. Yuan, J. Chen, J. Zeng, S. Tan, Preparation of monodisperse carbon nanospheres for electrochemical capacitors, Electrochem. Commun. 10 (2008) 1067.
[30] M.M. Titirici, M. Antonietti, N. Baccile, Hydrothermal carbon from biomass: a comparison of the local structure from poly- to monosaccharides and pentoses/hexoses, Green Chem. 10 (2008) 1204.
[31] S. Idesh, S. Kudo, K. Norinaga, J. Hayashi, Catalytic hydrothermal reforming of water-soluble organics from the pyrolysis of biomass using a Ni/carbon catalyst impregnated with Pt, Energ. Fuels 26 (2012) 67.
[32] S.A. Wohlgemuth, R.J. White, M.G. Willinger, M.M. Titirici, M. Antonietti, A one-pot hydrothermal synthesis of sulfur and nitrogen doped carbon aerogels with enhanced electrocatalytic activity in the oxygen reduction reaction, Green Chem. 14 (2012) 1515.

[33] L. Wei, M. Sevilla, A.B. Fuertes, R. Mokaya, G. Yushin, Hydrothermal carbonization of abundant renewable natural organic chemicals for high-performance supercapacitor electrodes, Adv. Energy Mater. 1 (2011) 356.
[34] L. Zhao, L.Z. Fan, M.Q. Zhou, H. Guan, S.Y. Qiao, M. Antonietti, M.M. Titirici, Nitrogen-containing hydrothermal carbons with superior performance in supercapacitors, Adv. Mater. 22 (2010) 5202.
[35] X.Y. Chen, C. Chen, Z.J. Zhang, D.H. Xie, X. Deng, J.W. Liu, Nitrogen-doped porous carbon for supercapacitor with long-term electrochemical stability, J. Power Sources 230 (2013) 50.
[36] M.M. Titirici, M. Antonietti, Chemistry and materials options of sustainable carbon materials made by hydrothermal carbonization, Chem. Soc. Rev. 39 (2010) 103.
[37] M. Wu, P. Ai, M. Tan, B. Jiang, Y. Li, J. Zheng, W. Wu, Z. Li, Q. Zhang, X. He, Synthesis of starch-derived mesoporous carbon for electric double layer capacitor, Chem. Eng. J. 245 (2014) 166.
[38] Y.W. Zhu, S. Murali, M.D. Stoller, K.J. Ganesh, W.W. Cai, P.J. Ferreira, A. Pirkle, R. M. Wallace, K.A. Cychosz, M. Thommes, D. Su, E.A. Stach, R.S. Ruoff, Carbon-based supercapacitors produced by activation of graphene, Science 332 (2011) 1537.
[39] M. Wu, Q. Zha, J. Qiu, Y. Guo, H. Shang, Preparation and characterization of porous carbons from PAN-based preoxidized cloth by KOH activation, Carbon 42 (2014) 205.
[40] D. Hulicova-Jurcakova, M. Seredych, G.Q. Lu, T.J. Bandosz, Combined effect of nitrogen- and oxygen-containing functional groups of microporous activated carbon on its electrochemical performance in supercapacitors, Adv. Funct. Mater. 19 (2009) 438.
[41] W. Ding, Z. Wei, S. Chen, X. Qi, T. Yang, J. Hu, D. Wang, S.F. Li Wan, Alvi, L. Li, Space-confinement-induced synthesis of pyridinic-and pyrrolic-nitrogen-doped graphene for the catalysis of oxygen reduction, Angew. Chem. Int. Ed. 52 (2013) 11755.
[42] Z. Li, Z.W. Xu, X.H. Tan, H.L. Wang, C.M.B. Holt, T. Stephenson, B.C. Olsen, D. Mitin, Mesoporous nitrogen-rich carbons derived from protein for ultra-high capacity battery anodes and supercapacitors, Energy Environ. Sci. 6 (2013) 871.
[43] P. Tammela, H. Olsson, M. Strømme, L. Nyholm, The influence of electrode and separator thickness on the cell resistance of symmetric cellulose-polypyrrole-based electric energy storage devices, J. Power Sources 272 (2014) 468.
[44] H. Zhu, J. Yin, X.L. Wang, H.Y. Wang, X.R. Yang, Microorganism-derived heteroatom-doped carbon materials for oxygen reduction and supercapacitors, Adv. Funct. Mater. 23 (2013) 1305.
[45] X. He, P. Ling, J. Qiu, M. Yu, X. Zhang, C. Yu, M. Zheng, Efficient preparation of biomass-based mesoporous carbons for supercapacitors with both high energy density and high power density, J. Power Sources 240 (2013) 109.
[46] X. Fan, C. Yu, Z. Ling, J. Yang, J. Qiu, Hydrothermal synthesis of phosphate-functionalized carbon nanotube-containing carbon composites for supercapacitors with highly stable performance, ACS Appl. Mater. Interfaces 5 (2013) 2104.